Renewable Energy 191 (2022) 662–668

Contents lists available at ScienceDirect

Renewable Energy

journal homepage: www.elsevier.com/locate/renene

Radiative cooling of solar cells with micro-grating photonic cooler

Bin Zhao [a, *], Kegui Lu [a], Mingke Hu [b], Jie Liu [a], Lijun Wu [a], Chengfeng Xu [a], Qingdong Xuan [c], Gang Pei [a, **]

[a] Department of Thermal Science and Energy Engineering, University of Science and Technology of China, Hefei, 230027, China
[b] Department of Architecture and Built Environment, University of Nottingham, University Park, Nottingham, NG7 2RD, UK
[c] School of Automotive and Transportation Engineering, Hefei University of Technology, 193 Tunxi Road, Hefei, 230009, China

ARTICLE INFO

Article history:
Received 17 February 2022
Received in revised form
6 April 2022
Accepted 10 April 2022
Available online 12 April 2022

Keywords:
Radiative cooling
Solar cells
Atmospheric window
Thermal emission
Photonic crystal

ABSTRACT

Radiative cooling of solar cells has been proposed in recent years and has elicited much interest from fields of materials science to engineering science. Herein, a silica micro-grating photonic cooler is proposed, designed, and fabricated to radiatively cool solar cells. It is shown that the micro-grating silica can not only improve the thermal emissivity of the bulk silica to over 0.9 required for enhanced radiative cooling of solar cells but also exhibits a slight anti-reflection effect for sunlight. The outdoor experiment demonstrates that the proposed cooler can passively reduce the temperature of the commercial silicon cell by 3.6 °C when applied on the top of the cell under solar irradiance range from approximately 830 W m^{-2} to 990 W m^{-2}, even though the cell already possesses a strong thermal emissivity of 0.67 and such a cooler slightly enhance the light trapping effect of the cell. This work provides an alternative way to design the solar-transparent infrared-emissive cooler for enhanced radiative cooling of solar cells and shows its cooling potential.

1. Introduction

Photovoltaic conversion has been recognized as one of the promising renewable energy techniques to eliminate the environmental issues (e.g., carbon emission and global warming) associated with the massive use of fossil fuels. Solar cells are the core of photovoltaic conversion, which can generate clean electricity from the sunlight directly. However, the power conversion efficiency of solar cells is limited at a level of approximately 20–30%. Besides, the potential conversion efficiency of a single junction solar cell was predicted to be approximately 30% based on the detailed balance analysis [1]. Importantly, a silicon solar cell absorbs incident sunlight strongly with an effective absorptivity over 0.9 [2], so nearly 60% of incident sunlight is dissipated into heat and then heats up the solar cell, which consequently harms the solar cell's power conversion performance and reduces its lifetime and reliability. Thus, effective cooling of solar cells is crucially required for photovoltaic conversion.

Currently, widely used cooling approaches for solar cells are relevant to conduction and convection, such as using metal heat sinks, forced cooling air/water [3,4], water immersing/spraying [5], and heat pipe cooling [6]. However, most of these methods generally require extra energy input or customized cooling structures, which increase the complexity of the system as well as increase the cost. Apart from conduction and convection, radiation is also a vital heat transfer mode for efficient cooling. Radiative cooling has been exactly one of the interesting passive cooling methods, which cools objects by pumping their heat into the cold universe in the form of thermal radiation, mainly relying on the transparency of the atmospheric window from 8 to 13 μm [7–13]. A variety of spectrally selective coolers have been developed and demonstrated to provide efficient cooling effects, such as multilayer films [14,15], photonic coolers [16,17], metamaterials [18,19], porous polymers [20,21], and advanced paints [22–24], which attracts much attention from the fields of material science and engineering. Recently, the idea of radiative cooling of solar cells has been proposed and investigated, and many reported researches have proved its possibility and demonstrated the cooling effect for solar cells in real-world conditions [25–29]. Bare silicon cells were theoretically and experimentally demonstrated to be cooled effectively after covering radiative coolers. For example, Zhu et al. designed a pyramid-structure-based cooler [27] and air holes-

* Corresponding author.
** Corresponding author.
E-mail addresses: zb630@ustc.edu.cn (B. Zhao), peigang@ustc.edu.cn (G. Pei).

https://doi.org/10.1016/j.renene.2022.04.063
0960-1481/

based photonic cooler [28] for radiative cooling of bare silicon cells, which shows that the bare cell can be passively cooled by over 10 °C under 1 sun conditions. Besides, pyramid-based photonic coolers are also good candidates for radiative cooling of solar cells [30–32], such as polydimethylsiloxane texture coolers [32]. If solar cells are under concentrated sunlight, the cooling effect will be further amplified. Peter et al. [33] demonstrated that the GaSb cell under 13 suns concentration can be radiatively cooled by 10 °C, which increases the open-circuit voltage by 5.7% and the lifetime increase is also predicted to be 40%. Moreover, the same group proposed a new structure for radiative cooling of concentrating photovoltaic based on GaSb cell, which experimentally demonstrates a temperature drop of 36 °C for PV cell, corresponding to a 31% increase of open-circuit voltage and 4–15 times predicted lifetime extension [34].

In this paper, we propose a silica micro-grating photonic cooler (refer to as "Grating silica" hereinafter) for enhanced radiative cooling of solar cells. A micro-grating structure with a periodicity of 7 μm is fabricated by the etching process. The duty ratio of the grating silica is 0.2 and the etching depth is 10 μm. Optical characterization shows that the grating silica is highly transparent to sunlight and has strong thermal emission in the mid-infrared wavelength regions with an average emissivity of 0.9. The outdoor experiment demonstrates that the commercial silicon cell can be cooled by over 3.6 °C after adding the grating silica on the top. To further explore the potential of radiative cooling of solar cells, model analysis is conducted by considering the effect of cooler, ambient parameters, and solar cells.

2. Results and discussion

2.1. The design, fabrication, and characterization of the cooler

The basic approach to enhance radiative cooling of solar cells is to place a radiative cooler on the top of the solar cell. In order to satisfy the requirement of photovoltaic conversion and radiative cooling, the radiative cooler needs to meet the following spectral criteria (Fig. 1a): First, the radiative cooler needs to have high solar transmittance for photovoltaic conversion, so materials with optical lossless properties are preferred for the radiative cooler. Second, the radiative cooler should exhibit strong thermal emission for enhanced radiative cooling, thus mid-infrared lossy materials with non-zero extinction coefficients are good candidates. Here, we propose a grating silica for enhanced radiative cooling of solar cells (Fig. 1b). Silica material is solar transparent and has high thermal emissivity in the thermal radiation band, which has been used in previous studies for sub-ambient radiative cooling [35,36]. The micro-grating structure is designed to overcome the impedance mismatch at the interface between the silica and ambient air and then reduce the strong reflectivity of the planar silica layer within the atmospheric window, corresponding to an emissivity improvement.

As illustrated in Fig. 1b, four parameters, i.e., grating periodicity p, grating width w, grating depth d, and cooler thickness t are used to describe the characteristic of the grating silica. Besides, the duty ratio r of the grating is expressed as $r = w/p$, which is an important variable for structure design. Here, the thickness t of the grating silica is selected as 500 μm since it is thin for the solar cell application and it is a kind of commercial size for silica material (i.e., silica wafer). Importantly, 500 μm is thicker enough than the effective depth penetration of the mid-infrared electromagnetic wave in silica. During the structure design, the average emissivity of the grating silica within the atmospheric window is selected as one of the vital indicators to evaluate the availability of the grating structure since there exists a huge emissivity drop for bulk silica due to its negative permittivity. Besides, the average transmittance of the grating silica within the wavelength range from 0.3 to 1.1 μm is another essential indicator because the effective optical efficiency of the cooler is the most important part of photovoltaic power generation. Rigorous coupled-wave analysis (RCWA) is applied to calculate the spectral responses of the grating silica, including reflectivity, transmittance, and emissivity [37]. The optical constant of the silica was obtained from the reference (Fig. S1) [38]. For calculation and optimization, considering the wavelength region of interest is 8–13 μm, the range of the p is selected to be between 5 and 15 μm, and the grating depth d is chosen to be between 5 and 25 μm. Besides, the duty ratio of the grating is within 0.1–0.9 with a step of 0.1. After considering the above optical requirements and the complexity of the grating structure, parameter combination (p, r, d) is selected as (7 μm, 0.2, 10 μm) and the spectral response of the grating silica and 500-μm-thick planar silica are presented in Fig. 1c. The planar silica has a strong emissivity drop within the atmospheric window and the micro-grating structure well improves the emissivity and exhibits an average emissivity of approximately 0.9. Importantly, the predicted transmittance of the planar silica and grating silica is nearly the same, which indicates that the micro-grating structure does not degrade the optical property of the silica in the solar radiation band.

For experimental demonstration, the designed grating silica is fabricated (Fig. 2a) and characterized. Fig. 2b shows the top and cross-section views of the grating silica, which matches well with the designed structure. The spectral emissivity of the silicon cell with grating silica (i.e., grating silica in Fig. 2c), silicon cell with planar silica (i.e., planar silica in Fig. 2c), and bare silicon cell (i.e., bare case in Fig. 2c) are measured. The absorptivity ($\alpha_{0.3\text{-}1.1}$) of the cell w/o silica on the top within the wavelength band of 0.3–1.1 μm is nearly the same (Fig. 2c) with an average absorptivity of approximately 0.95 and a slight absorption improvement of the cell after adding grating silica (Fig. 2d) due to its anti-reflection effect is observed. The I–V testing results also prove the existence of the anti-reflection effect (Fig. S2). In the mid-infrared wavelength band, the emissivity of the cell with grating silica is the highest with an average emissivity of 0.91, while the emissivity of the bare cell and the cell with planar silica are 0.67 and 0.81, respectively. Importantly, the emissivity drop of the planar silica near 9 μm is almost eliminated by the designed grating photonic structure, which is a good feature for radiative cooling of solar cells. Meanwhile, the infrared photos (Fig. 2e) also reveal the thermal emissivity properties of the bare cell, the cell with planar silica, and the cell with grating silica due to the positive correlative relationship between the apparent temperature of the surface and its emissivity. To further demonstrate the emissivity improvement of the grating silica, the stagnation temperatures of the silicon cell, the cell with grating silica, and the cell with planar silica are measured under a controlled solar simulator (Fig. S3), which shows the cell with grating silica is always the coldest among all three samples and its stagnation temperature is 10.0 °C and 2.5 °C lower than those of bare cell case and the cell with planar silica.

2.2. Modeling steady-state temperature of the solar cell

To analyze the radiative cooling effect of the grating silica on the solar cell, a thermal model is used for steady-state temperature prediction. We consider that the temperature of the solar cell with the grating silica is uniform since the integrated structure is thin and this assumption has also been used and approved. The energy balance of the solar cell is relevant to sunlight, atmosphere, ambient air, and the integrated solar cell (Fig. 3a). According to the first law of thermodynamics, the energy governing equation is expressed as:

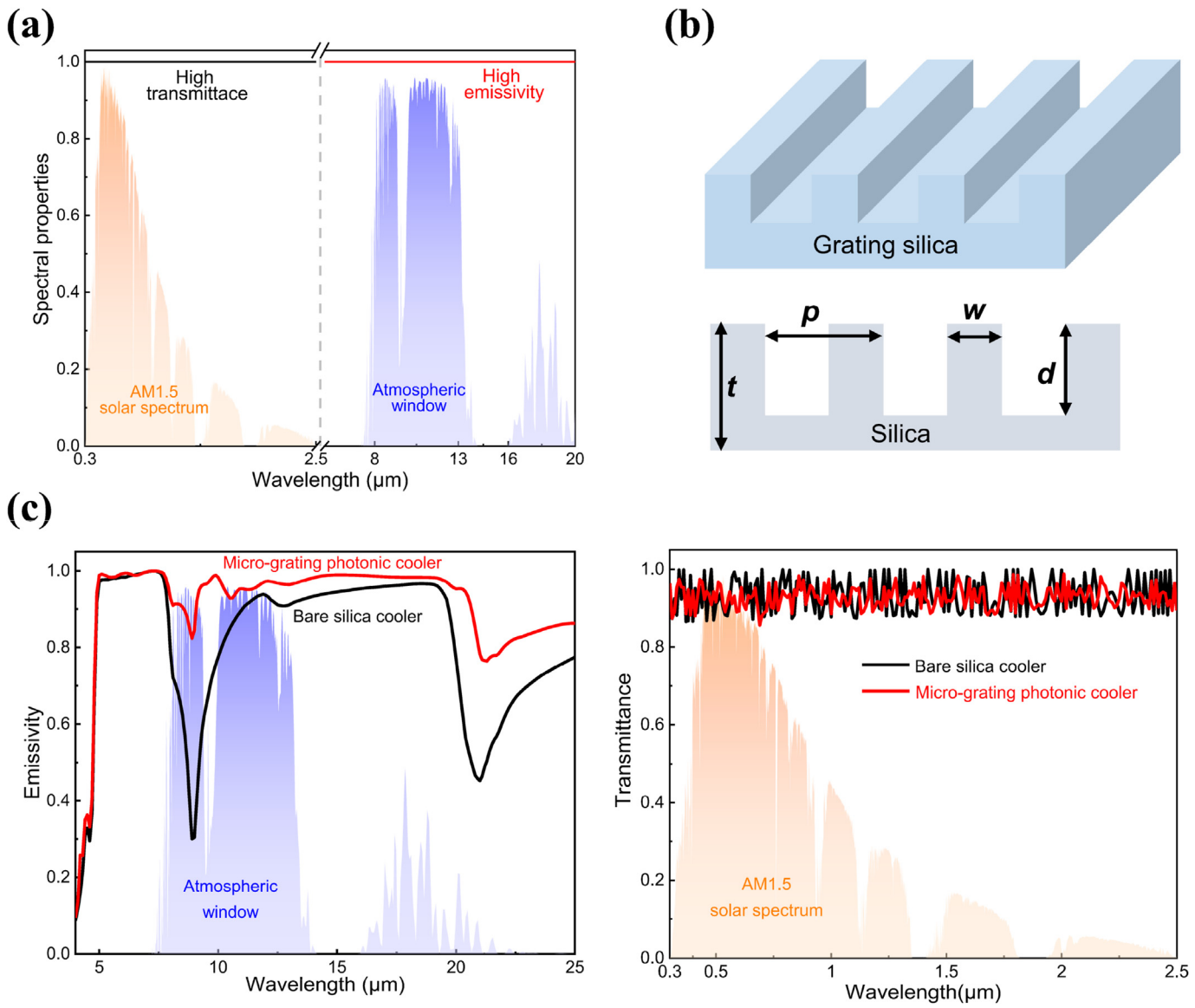

Fig. 1. (a) Ideal spectral transmittance and emissivity spectrum for the radiative cooler to cool solar cells. (b) Schematic of the proposed grating silica. Section-view of the grating silica with periodicity p, grating width w, grating depth d, and cooler thickness t, is presented as reference. (c) Simulated mid-infrared emissivity spectrum and solar transmittance spectrum of the planar silica and grating silica.

$$Q_{rad}(T_c) - Q_{sun} - Q_{atm}(T_a) + Q_{non\_rad}(T_c - T_a) = 0 \tag{1}$$

where T_c is cell temperature and T_a is ambient temperature, $Q_{rad}(T_c)$ is the radiative heat power of the solar cell w/o the grating silica and can be expressed as [39]:

$$Q_{rad}(T_c) = A \cdot 2\pi \int_0^{\infty} \int_0^{\frac{\pi}{2}} I_{BB}(\lambda,\ T_c)\varepsilon(\lambda,\ \theta)\ cos\theta\ sin\theta\ d\theta d\lambda \tag{2}$$

where I_{BB} is the spectral radiance density of a blackbody, $\varepsilon(\lambda, \theta)$ is the spectral angular emissivity of the solar cell w/o the grating silica, A is the area of the solar cell. The absorbed solar power Q_{sun} can be expressed as:

$$Q_{sun} = A \cdot G\alpha \tag{3}$$

where G is the total solar power flux and α is the AM 1.5 weighted solar absorptivity of the solar cell w/o the grating silica. The absorbed atmospheric heat power $Q_{atm}(T_a)$ can be expressed as [39]:

$$Q_{atm}(T_a) = A \cdot 2\pi \int_0^{\infty} \int_0^{\frac{\pi}{2}} I_{BB}(\lambda,\ T_a)\varepsilon(\lambda,\ \theta)\varepsilon_{atm}(\lambda,\ \theta)\ cos\theta\ sin\theta\ d\theta d\lambda \tag{4}$$

where $\varepsilon(\lambda, \theta)$ is the spectral angular emissivity of the atmosphere and can be estimated using a correlation [14] $\varepsilon(\lambda, \theta) = 1\text{-}\tau(\lambda, 0)^{1/\cos\theta}$, $\tau(\lambda, 0)$ is the transmittance of the atmosphere in the zenith direction. The heat flux caused by convection and conduction heat transfer modes, represented as $P_{non\_rad}(T_c, T_a)$, can be described using an overall heat transfer coefficient h_c:

$$Q_{non\_rad}(T_c,\ T_a) = A \cdot h_c(T_c - T_a) \tag{5}$$

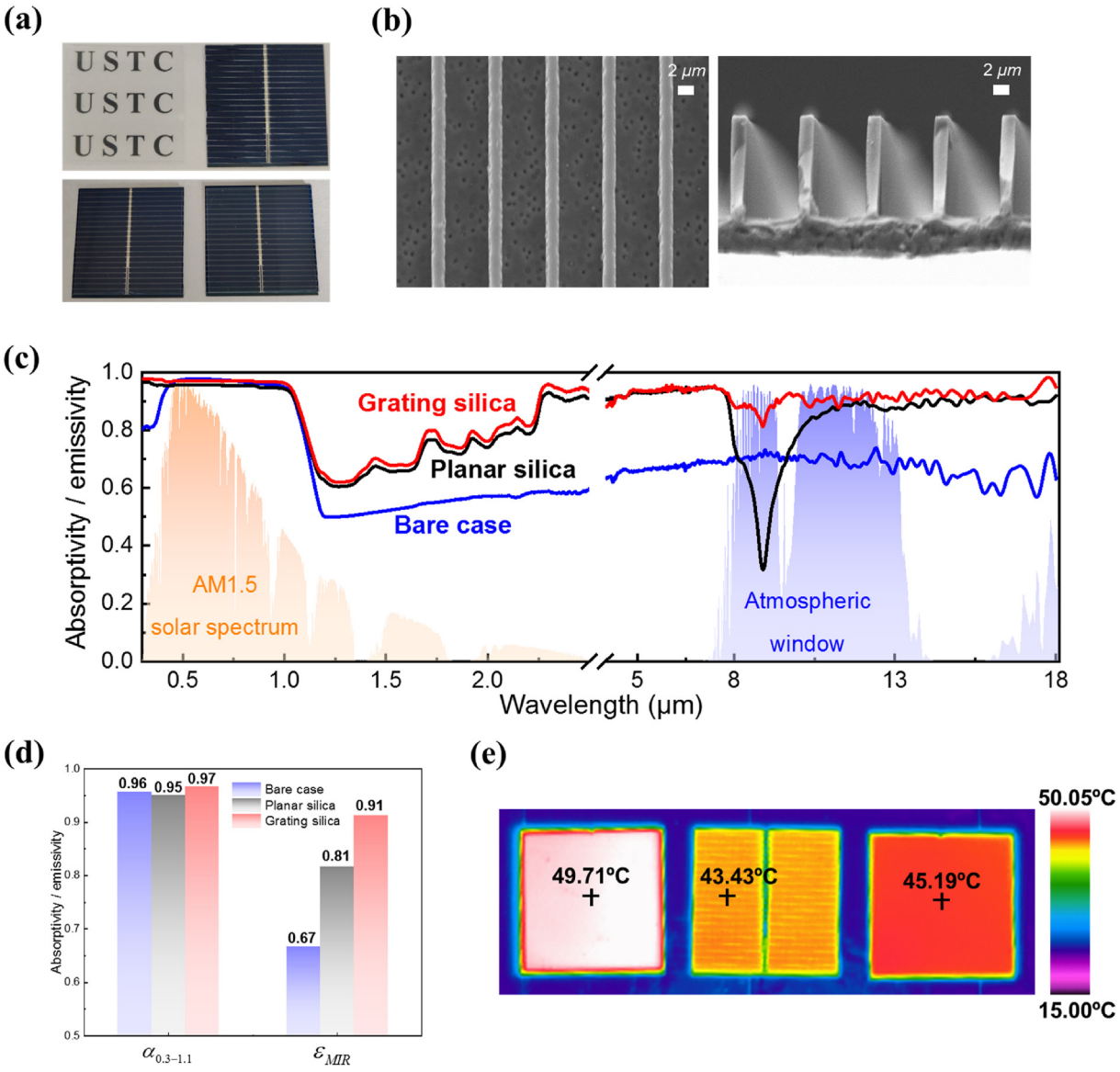

Fig. 2. (a) Optical images of grating silica, bare silicon cell, the cell with planar silica, and the cell with grating silica. (b) Top-view and cross-section view scanning electron microscope (SEM) images of the grating silica. (c) Measured solar absorptivity and thermal emissivity of the bare cell, the cell with planar silica, and the cell with grating silica. (d) Average absorptivity within the 0.3–1.1 μm and average emissivity in the mid-infrared wavelength band. (e) Infrared images of the bare cell, the cell with planar silica, and the cell with grating silica at a testing temperature of 52.5 °C.

During simulation, the spectral atmospheric transmittance is obtained from the MODTRAN [40]. Besides, ambient temperature is set as 300 K, and the overall heat transfer coefficient is set to be 6 W m^{-2} K^{-1}, corresponding to the wind speed of approximately 2 m s^{-1}. Notably, a 200-μm-thick silicon is selected as the solar cell in this section to purely evaluate the radiative cooling performance of the grating silica and the solar absorption and thermal emission of the cell w/o the grating silica are theoretically simulated (Fig. S4).

Bare silicon cell is heated up by the sunlight under various solar irradiances and operates at 77.5 °C above ambient temperature under 800 W m^{-2} solar irradiance (Fig. 3b). However, the solar cell with the grating silica added operates at 37.5 °C above ambient temperature under 800 W m^{-2}, showing that the grating silica can passively cool the solar cell by 40 °C using radiative cooling. It is noted that such a cooling effect may be overestimated since the bare silicon cell has little thermal emission within the mid-infrared band, but it does demonstrate the feasibility of the radiative cooling of solar cells. For above-ambient heat dissipation conditions, the non-radiative heat transfer mode also plays an essential role. As shown in Fig. 3c, the temperature of the solar cell w/o the grating silica decreases dramatically with the increase of h, and the temperature difference of the solar cell with and without the grating silica also reduces. At $h = 4$ W m^{-2} K^{-1}, the temperature of the solar cell w/o the grating silica is 119.0 °C and 61.0 °C, indicating that the grating silica results in a cell temperature reduction of 58 °C. When h increases to 20 W m^{-2} K^{-1}, the solar cell w/o the grating silica operates at 45.6 °C and 40.5 °C, respectively, corresponding to the temperature difference of 5.1 °C. This scenario is caused by the relative change of thermal resistance during the convection and radiation coupled heat transfer process.

2.3. Outdoor radiative cooling of solar cells

To further evaluate the radiative cooling performance of the grating silica on solar cells, an outdoor experimental demonstration

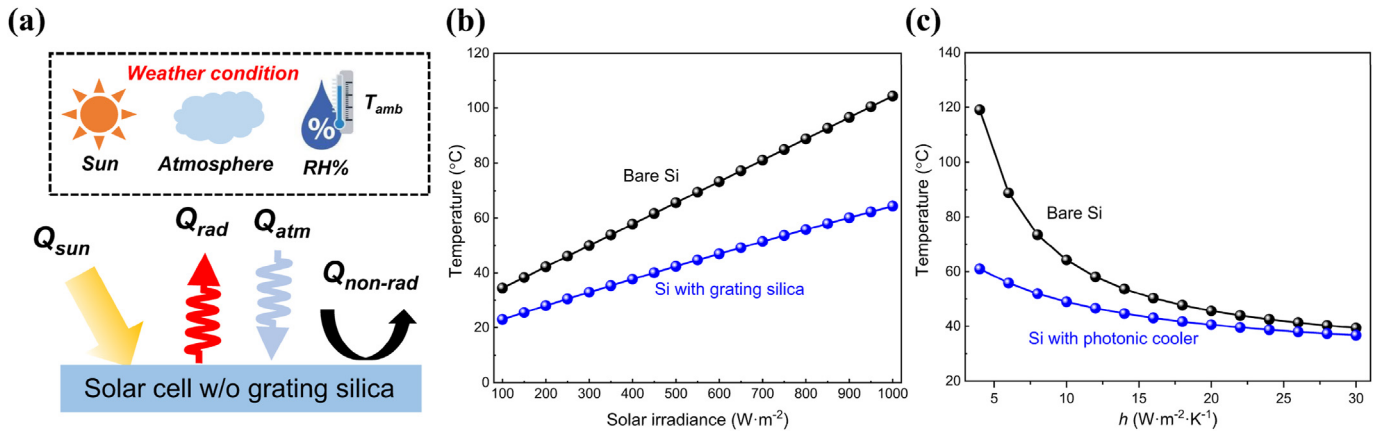

Fig. 3. (a) Energy balance of the silicon cell w/o the grating silica, which involves absorbed solar power Q_{sun}, radiated thermal emission power Q_{rad}, absorbed thermal emission power from the atmosphere Q_{atm}, and non-radiative power $Q_{non\text{-}rad}$. (b)–(c) Predicted solar cell temperature under different solar irradiance and h.

is conducted on April 03, 2022. The experimental setup described in Fig. 4a and b mainly consists of an acrylic chamber, polystyrene materials, polyethylene (PE) film, aluminum (Al) foils, and a metal frame. The solar cell w/o the cooler is placed on top of polystyrene that has low thermal conductivity and then fixed in the acrylic chamber. The top surfaces of the chamber and polystyrene are all covered by Al foils to reduce their parasitic solar absorption and thermal radiation. The PE film is used to decouple the sample with ambient air so that the radiative cooling effect of the grating silica can be investigated individually.

The temperatures of the bare silicon cell, the cell with planar silica, and the cell with grating silica are measured and presented in

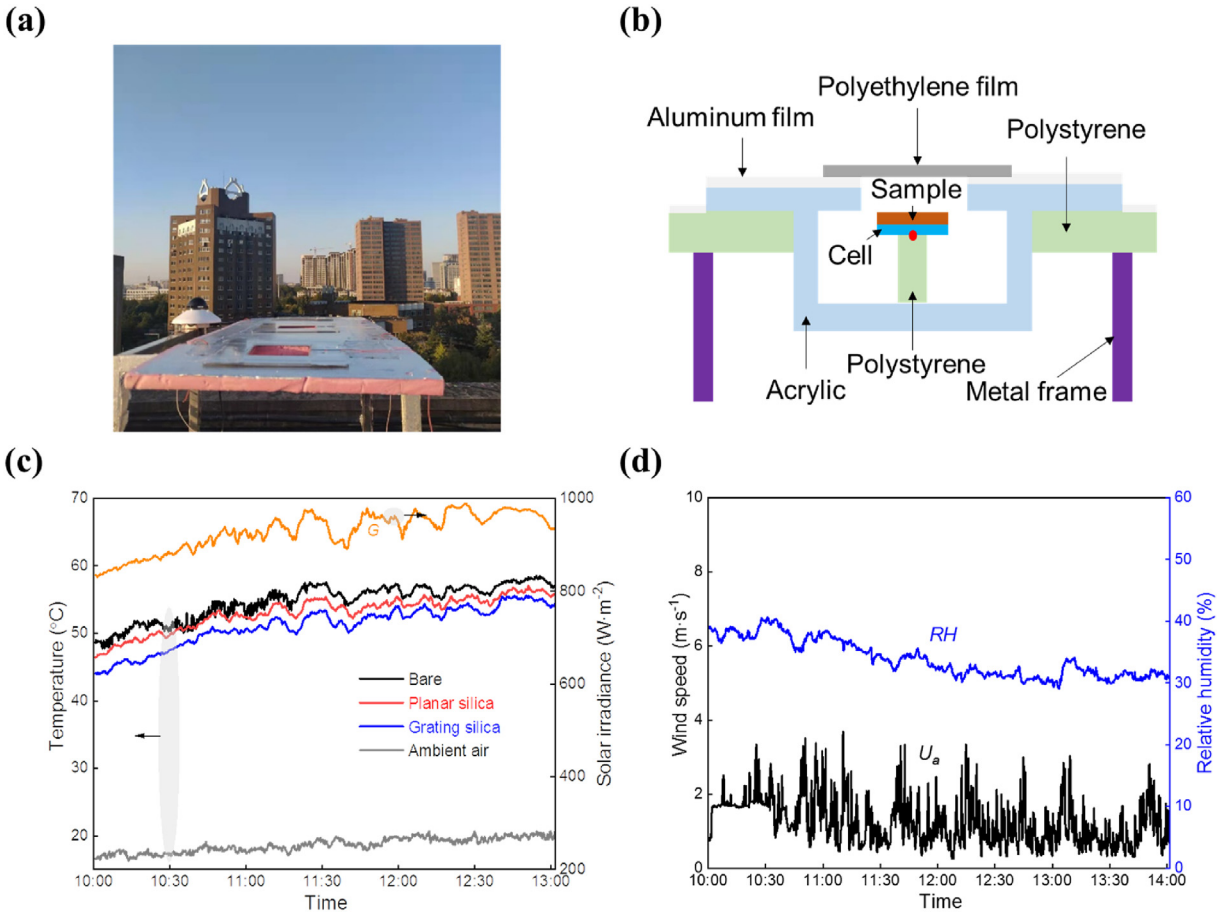

Fig. 4. Outdoor experimental demonstration with a PE convection shield covered. (a) Photo of the experimental setup. (b) Schematic of the experimental setup. Bare silicon cell, the cell with planar silica, and the cell with grating silica are placed on top of polystyrene that has low thermal conductivity. The red point inserted in the figure is the thermocouple position. (c) Measured temperature of the bare silicon cell, the cell with planar silica, and the cell with grating silica, with ambient temperature and solar irradiance (i.e., G) plotted as references. (d) Measured wind speed (i.e, U_a) and relative humidity (RH) of the local environment during the testing period.

Fig. 4c with ambient air temperature and solar irradiance plotted as references, and the measured data is also applied for the model validation (Fig. S5). During the testing, solar irradiance varies from approximately 830 W m^{-2} to 990 W m^{-2}, and the temperature of the cell with grating silica is always the lowest, while the temperature of the bare cell is maintained at the highest condition. Specifically, the arithmetic averaged temperature of the cell with grating silica is 3.6 °C lower than that of the bare cell even though the AM1.5 weighted solar absorptivity of the former is obviously greater than that of the latter (Fig. 2c), indicating that the grating silica is a good candidate of the transparent cooler for enhanced radiative cooling of solar cells. Moreover, the cell with grating silica is also 2.0 °C cooler on average than that of the cell with planar. Compared with the reported results of temperature reduction (e.g. over 10 °C after using the cooler [27]) on this topic, a temperature reduction of 3.6 °C may be overshadowed, but it needs to be highlighted that the bare cell used in this work is a commercial silicon cell that already has a strong thermal emission rather than bare or doped silicon whose emissivity is maintained at a relatively low level. If the strong reflection of near-infrared light is considered for the cooler, the cooling performance of the cooler will be further improved, and adding multilayer solar splitting film is one of the possible methods [41].

Notably, solar cells are exposed to ambient air directly on the photovoltaic applications level, so radiation heat transfer and convection heat transfer of solar cells occur simultaneously. Thus, the temperature of different samples with the silicon solar cell is also measured without PE cover (Fig. S6), which shows the temperature of the solar cell with grating silica is also lower than that of the bare silicon cell with an arithmetic averaged temperature reduction of approximately 1.8 °C, indicating the enhanced radiative cooling effect of the proposed grating silica. Moreover, it should be pointed out that glass cover is widely used for commercial photovoltaic modules. Here, a universal and possible route for radiative cooling of PV modules is copying the micro-grating structure to the bulk glass material that contains approximately 70% of silica and 30% other constituents (e.g., Na_2O, CaO, MgO) [42] and re-design the characteristic parameters for micro-grating structure (Fig. S7).

3. Conclusions

In this paper, a grating silica is designed and fabricated to radiatively cool solar cells. The micro-grating structure has a periodicity of 7 μm, a duty ratio of 0.2, and a vertical depth of 10 μm. The proposed silica grating not only improves the thermal emissivity of the solar cell to approximately 0.9 but also reinforces the light trapping effect of the solar cell for power generation enhancement. When exposed to the outdoor environment, the commercial silicon cell that already has an average emissivity of nearly 0.67 can still be passively cooled by 3.6 °C after adding the grating silica on the top, showing the cooling potential of radiative cooling mechanism for thermal management of solar cells.

4. Experimental methods

4.1. Fabrication of the cooler

A 550-nm-thick aluminum film is deposited on a quartz substrate with a thickness of 500 μm and a layer of 1-μm-thick photoresist (AZ6112) is spin-coated on the aluminum film at 3000 rpm and 100 °C for 90 s. Then, the maskless lithography of the sample is performed using the direct-write lithography machine (ATD1500, Advantools Co., Ltd.) under 66 mW, and the sample is then developed by immersion in a developer (AZ 300 MIF) for 35s with a subsequent deionized water washing. Next, the sample is baked at 110 °C for 120s (hard baking). Next, the aluminum film is etched off by an ICP etching machine (Plasma System100 ICP180, Oxford), and nearly 10-μm-thick quartz is then etched off by an ICP (Plasma System100 ICP380, Oxford) at a pressure of 4.0 mTorr (gas compositions: 40 sccm C_4F_8, 10 sccm O_2, 80 sccm RF). During the etching process, multiple cool-downs are required to prevent overheating of the sample.

4.2. Optical, electrical, and structural characterization

Solar transmittance spectrums of the micro-grating silica cooler and bulk silica are measured by a UV–Vis–NIR spectrometer (SolidSpec-3700 DUV, Shimadzu) equipped with a Teflon coated integrating sphere. The spectral reflectivity spectrums of the samples in the MIR wavelength band are measured by a Fourier transform infrared spectrometer (Nicolet iS 50, Thermo Scientific) equipped with a gold-coated integrating sphere. The current-voltage (I–V) curve is measured using a solar simulator (Oriel Sol3A Class AAA, Newport) with a light intensity of 1000 W/m^2 under AM1.5G illumination. The cross-sectional morphologies of the micro-grating silica cooler are obtained by scanning electron microscopy (EVO 18, Zeiss). The IR images of the bare cell, the cell with planar silica, and the cell with grating silica are obtained by a radiometric thermographic system (VarioCAM® hr head, InfraTec).

4.3. Thermal performance measurements

During the outdoor experimental testing, the experimental setup (Fig. 4a) is fixed horizontally and the temperature values of samples are measured by the T-type thermocouples that are fixed on the backside of samples with an uncertainty of ±0.5 °C. Total solar radiation is measured by a pyranometer (TBQ-2, Jinzhou Sunshine Technology Co., Ltd) that is installed in parallel with samples with an uncertainty of ±2%. Moreover, ambient temperature and relative humidity are measured using an integrated weather station (HSTL-BYXWS). All above-mentioned data are collected and recorded using a data acquisition instrument (LR8450, HIOKI).

Data availability

The data that support the findings of this study are available from the corresponding author upon reasonable request.

Declaration of competing interest

The authors declare that they have no known competing financial interests or personal relationships that could have appeared to influence the work reported in this paper.

Acknowledgments

This work was supported by the National Natural Science Foundation of China (NSFC 52106276, 52130601, and 51906241), Project funded by China Postdoctoral Science Foundation (2020TQ0307 and 2020M682033), Fundamental Research Funds for the Central Universities (WK2090000028), and Research center for multi-energy complementation and conversion of USTC. We thank the USTC Center for Micro and Nanoscale Research and Fabrication for its help in grating silica fabrication and thank Dr. Cheng Chen for his help on Infrared image testing.

Appendix A. Supplementary data

Supplementary data to this article can be found online at https://doi.org/10.1016/j.renene.2022.04.063.

References

[1] W. Shockley, H.J. Queisser, Detailed balance limit of efficiency of p-n junction solar cells, J. Appl. Phys. 32 (1961) 510–519, https://doi.org/10.1063/1.1736034.

[2] B. Zhao, M. Hu, X. Ao, G. Pei, Performance analysis of enhanced radiative cooling of solar cells based on a commercial silicon photovoltaic module, Sol. Energy 176 (2018) 248–255, https://doi.org/10.1016/j.solener.2018.10.043.

[3] A.S. Kaiser, B. Zamora, R. Mazón, J.R. García, F. Vera, Experimental study of cooling BIPV modules by forced convection in the air channel, Appl. Energy 135 (2014) 88–97, https://doi.org/10.1016/j.apenergy.2014.08.079.

[4] Y. Zhang, C. Shen, C. Zhang, J. Pu, Q. Yang, C. Sun, A novel porous channel to optimize the cooling performance of PV modules, Energy Built. Environ. 3 (2022) 210–225, https://doi.org/10.1016/j.enbenv.2021.01.003.

[5] M. Abdolzadeh, M. Ameri, Improving the effectiveness of a photovoltaic water pumping system by spraying water over the front of photovoltaic cells, Renew. Energy 34 (2009) 91–96, https://doi.org/10.1016/j.renene.2008.03.024.

[6] P. Gang, F. Huide, Z. Huijuan, J. Jie, Performance study and parametric analysis of a novel heat pipe PV/T system, Energy 37 (2012) 384–395, https://doi.org/10.1016/j.energy.2011.11.017.

[7] B. Zhao, M. Hu, X. Ao, N. Chen, G. Pei, Radiative cooling: a review of fundamentals, materials, applications, and prospects, Appl. Energy 236 (2019) 489–513, https://doi.org/10.1016/j.apenergy.2018.12.018.

[8] D. Zhao, A. Aili, Y. Zhai, S. Xu, G. Tan, X. Yin, R. Yang, Radiative sky cooling: Fundamental principles, materials, and applications, Appl. Phys. Rev. 6 (2019), 021306, https://doi.org/10.1063/1.5087281.

[9] T. Li, Y. Zhai, S. He, W. Gan, Z. Wei, M. Heidarinejad, D. Dalgo, R. Mi, X. Zhao, J. Song, J. Dai, C. Chen, A. Aili, A. Vellore, A. Martini, R. Yang, J. Srebric, X. Yin, L. Hu, A radiative cooling structural material, Science 364 (2019) 760–763, https://doi.org/10.1126/science.aau9101.

[10] W. Li, S. Fan, Radiative cooling: harvesting the coldness of the universe, Opt Photon. News 30 (2019) 32, https://doi.org/10.1364/OPN.30.11.000032.

[11] S. Fan, A. Raman, Metamaterials for radiative sky cooling, Natl. Sci. Rev. 5 (2018) 132–133, https://doi.org/10.1093/nsr/nwy012.

[12] Z. Cheng, Y. Shuai, D. Gong, F. Wang, H. Liang, G. Li, Optical properties and cooling performance analyses of single-layer radiative cooling coating with mixture of TiO_2 particles and SiO_2 particles, Sci. China Technol. Sci. 64 (2021) 1017–1029, https://doi.org/10.1007/s11431-020-1586-9.

[13] C. Lin, Y. Li, C. Chi, Y.S. Kwon, J. Huang, Z. Wu, J. Zheng, G. Liu, C.Y. Tso, C.Y.H. Chao, B. Huang, A solution-processed inorganic emitter with high spectral selectivity for efficient subambient radiative cooling in hot humid climates, Adv. Mater. 2109350 (2022), 2109350, https://doi.org/10.1002/adma.202109350.

[14] A.P. Raman, M.A. Anoma, L. Zhu, E. Rephaeli, S. Fan, Passive radiative cooling below ambient air temperature under direct sunlight, Nature 515 (2014) 540–544, https://doi.org/10.1038/nature13883.

[15] H. Ma, K. Yao, S. Dou, M. Xiao, M. Dai, L. Wang, H. Zhao, J. Zhao, Y. Li, Y. Zhan, Multilayered SiO2/Si3N4 photonic emitter to achieve high-performance all-day radiative cooling, Sol. Energy Mater. Sol. Cells 212 (2020), 110584, https://doi.org/10.1016/j.solmat.2020.110584.

[16] E. Rephaeli, A. Raman, S. Fan, Ultrabroadband photonic structures to achieve high-performance daytime radiative cooling, Nano Lett. 13 (2013) 1457–1461, https://doi.org/10.1021/nl4004283.

[17] B. Zhao, M. Hu, X. Ao, Q. Xuan, G. Pei, Comprehensive photonic approach for diurnal photovoltaic and nocturnal radiative cooling, Sol. Energy Mater. Sol. Cells 178 (2018) 266–272, https://doi.org/10.1016/j.solmat.2018.01.023.

[18] Y. Zhai, Y. Ma, S.N. David, D. Zhao, R. Lou, G. Tan, R. Yang, X. Yin, Scalable-manufactured randomized glass-polymer hybrid metamaterial for daytime radiative cooling, Science 355 (2017) 1062–1066, https://doi.org/10.1126/science.aai7899.

[19] S. Zeng, S. Pian, M. Su, Z. Wang, M. Wu, X. Liu, M. Chen, Y. Xiang, J. Wu, M. Zhang, Q. Cen, Y. Tang, X. Zhou, Z. Huang, R. Wang, A. Tunuhe, X. Sun, Z. Xia, M. Tian, M. Chen, X. Ma, L. Yang, J. Zhou, H. Zhou, Q. Yang, X. Li, Y. Ma, G. Tao, Hierarchical-morphology metafabric for scalable passive daytime radiative cooling, Science 373 (2021) 692–696, https://doi.org/10.1126/science.abi5484.

[20] J. Mandal, Y. Fu, A.C. Overvig, M. Jia, K. Sun, N.N. Shi, H. Zhou, X. Xiao, N. Yu, Y. Yang, Hierarchically porous polymer coatings for highly efficient passive daytime radiative cooling, Science 362 (2018) 315–319, https://doi.org/10.1126/science.aat9513.

[21] D. Li, X. Liu, W. Li, Z. Lin, B. Zhu, Z. Li, J. Li, B. Li, S. Fan, J. Xie, J. Zhu, Scalable and hierarchically designed polymer film as a selective thermal emitter for high-performance all-day radiative cooling, Nat. Nanotechnol. 16 (2021) 153–158, https://doi.org/10.1038/s41565-020-00800-4.

[22] H. Bao, C. Yan, B. Wang, X. Fang, C.Y. Zhao, X. Ruan, Double-layer nanoparticle-based coatings for efficient terrestrial radiative cooling, Sol. Energy Mater. Sol. Cells 168 (2017) 78–84, https://doi.org/10.1016/j.solmat.2017.04.020.

[23] X. Li, J. Peoples, Z. Huang, Z. Zhao, J. Qiu, X. Ruan, Full daytime sub-ambient radiative cooling in commercial-like paints with high figure of merit, Cell Rep. Phys. Sci. 1 (2020), 100221, https://doi.org/10.1016/j.xcrp.2020.100221.

[24] Z. Cheng, H. Han, F. Wang, Y. Yan, X. Shi, H. Liang, X. Zhang, Y. Shuai, Efficient radiative cooling coating with biomimetic human skin wrinkle structure, Nano Energy 89 (2021), 106377, https://doi.org/10.1016/j.nanoen.2021.106377.

[25] B. Zhao, M. Hu, X. Ao, Q. Xuan, G. Pei, Spectrally selective approaches for passive cooling of solar cells: a review, Appl. Energy 262 (2020), 114548, https://doi.org/10.1016/j.apenergy.2020.114548.

[26] H. Tang, Z. Zhou, S. Jiao, Y. Zhang, S. Li, D. Zhang, J. Zhang, J. Liu, D. Zhao, Radiative cooling of solar cells with scalable and high-performance nano-porous anodic aluminum oxide, Sol. Energy Mater. Sol. Cells 235 (2022), 111498, https://doi.org/10.1016/j.solmat.2021.111498.

[27] L. Zhu, A. Raman, K.X. Wang, M.A. Anoma, S. Fan, Radiative cooling of solar cells, Optica 1 (2014) 32–38, https://doi.org/10.1364/OPTICA.1.000032.

[28] L. Zhu, A.P. Raman, S. Fan, Radiative cooling of solar absorbers using a visibly transparent photonic crystal thermal blackbody, Proc. Natl. Acad. Sci. Unit. States Am. 112 (2015) 12282–12287, https://doi.org/10.1073/pnas.1509453112.

[29] Z. Li, S. Ahmed, T. Ma, Investigating the effect of radiative cooling on the operating temperature of photovoltaic modules, Sol. RRL (2021), 202000735, https://doi.org/10.1002/solr.202000735 solr.

[30] Y. Lu, Z. Chen, L. Ai, X. Zhang, J. Zhang, J. Li, W. Wang, R. Tan, N. Dai, W. Song, A universal route to realize radiative cooling and light management in photovoltaic modules, Sol. RRL 1 (2017), 1700084, https://doi.org/10.1002/solr.201700084.

[31] E. Lee, T. Luo, Black body-like radiative cooling for flexible thin-film solar cells, Sol. Energy Mater. Sol. Cells 194 (2019) 222–228, https://doi.org/10.1016/j.solmat.2019.02.015.

[32] K. Wang, G. Luo, X. Guo, S. Li, Z. Liu, C. Yang, Radiative cooling of commercial silicon solar cells using a pyramid-textured PDMS film, Sol. Energy 225 (2021) 245–251, https://doi.org/10.1016/j.solener.2021.07.025.

[33] Z. Zhou, Z. Wang, P. Bermel, Radiative cooling for low-bandgap photovoltaics under concentrated sunlight, Opt Express 27 (2019) A404, https://doi.org/10.1364/OE.27.00A404.

[34] Z. Wang, D. Kortge, J. Zhu, Z. Zhou, H. Torsina, C. Lee, P. Bermel, Lightweight, passive radiative cooling to enhance concentrating photovoltaics, Joule 4 (2020) 2702–2717, https://doi.org/10.1016/j.joule.2020.10.004.

[35] J. Kou, Z. Jurado, Z. Chen, S. Fan, A.J. Minnich, Daytime radiative cooling using near-black infrared emitters, ACS Photonics 4 (2017) 626–630, https://doi.org/10.1021/acsphotonics.6b00991.

[36] B. Zhao, M. Hu, X. Ao, G. Pei, Performance evaluation of daytime radiative cooling under different clear sky conditions, Appl. Therm. Eng. 155 (2019) 660–666, https://doi.org/10.1016/j.applthermaleng.2019.04.028.

[37] V. Liu, S. Fan, S4 : a free electromagnetic solver for layered periodic structures, Comput. Phys. Commun. 183 (2012) 2233–2244, https://doi.org/10.1016/j.cpc.2012.04.026.

[38] E.D. Palik, Handbook of Optical Constants of Solids, Academic press, 1985.

[39] T.L. Bergman, A.S. Lavine, F.P. Incropera, D.P. DeWitt, Fundamentals of Heat and Mass Transfer, Seventh, John Wiley & Sons, 2011.

[40] MODTRAN infrared light in the atmosphere. http://climatemodels.uchicago.edu/modtran/. (Accessed 1 November 2021).

[41] W. Li, Y. Shi, K. Chen, L. Zhu, S. Fan, A comprehensive photonic approach for solar cell cooling, ACS Photonics 4 (2017) 774–782, https://doi.org/10.1021/acsphotonics.7b00089.

[42] Soda-lime glass. https://en.wikipedia.org/wiki/Sodalime_glass. (Accessed 9 September 2021).